Neuroradiology (2013) 55:603–613
DOI 10.1007/s00234-013-1145-x

DIAGNOSTIC NEURORADIOLOGY

Utility of multiparametric 3-T MRI for glioma characterization

Bhaswati Roy · Rakesh K. Gupta · Andrew A. Maudsley · Rishi Awasthi · Sulaiman Sheriff · Meng Gu · Nuzhat Husain · Sudipta Mohakud · Sanjay Behari · Chandra M. Pandey · Ram K. S. Rathore · Daniel M. Spielman · Jeffry R. Alger

Received: 1 November 2012 / Accepted: 21 January 2013 / Published online: 2 February 2013

Abstract
Introduction Accurate grading of cerebral glioma using conventional structural imaging techniques remains challenging due to the relatively poor sensitivity and specificity of these methods. The purpose of this study was to evaluate the relative sensitivity and specificity of structural magnetic resonance imaging and MR measurements of perfusion, diffusion, and whole-brain spectroscopic parameters for glioma grading.

Methods Fifty-six patients with radiologically suspected untreated glioma were studied with T1- and T2-weighted MR imaging, dynamic contrast-enhanced MR imaging, diffusion tensor imaging, and volumetric whole-brain MR spectroscopic imaging. Receiver-operating characteristic analysis was performed using the relative cerebral blood volume (rCBV), apparent diffusion coefficient, fractional anisotropy, and multiple spectroscopic parameters to determine optimum thresholds for tumor grading and to obtain the sensitivity, specificity, and positive and negative predictive values for identifying high-grade gliomas. Logistic regression was performed to analyze all the parameters together.
Results The rCBV individually classified glioma as low and high grade with a sensitivity and specificity of 100 and 88 %, respectively, based on a threshold value of 3.34. On combining all parameters under consideration, the classification was achieved with 2 % error and sensitivity and specificity of 100 and 96 %, respectively.
Conclusion Individually, CBV measurement provides the greatest diagnostic performance for predicting glioma grade; however, the most accurate classification can be achieved by combining all of the imaging parameters.

Keywords Multiparametric MRI · Glioma grading · Dynamic contrast enhance MR · Whole-brain MRSI · Diffusion tensor imaging

B. Roy · R. K. Gupta (✉)
Department of Radiology & Imaging, Fortis Memorial Research Institute, Gurgaon, Haryana, India 122002
e-mail: rakeshree1@gmail.com

A. A. Maudsley · S. Sheriff
Department of Radiology, University of Miami, Miami, USA

R. Awasthi · S. Mohakud
Department of Radiodiagnosis, Sanjay Gandhi Postgraduate Institute of Medical Sciences, Lucknow, India

M. Gu · D. M. Spielman
Department of Radiology, Stanford University, Standford, USA

N. Husain
Department of Pathology, Ram Manohar Lohia Institute of Medical Sciences, Lucknow, India

S. Behari
Department of Neurosurgery, Sanjay Gandhi Postgraduate Institute of Medical Sciences, Lucknow, India

C. M. Pandey
Department of Biostatistics & Health Informatics, Sanjay Gandhi Postgraduate Institute of Medical Sciences, Lucknow, India

R. K. S. Rathore
Department of Mathematics & Statistics,
Indian Institute of Technology, Kanpur, India

J. R. Alger
Department of Radiological Sciences, UCLA School of Medicine, Los Angeles, USA

Introduction

Gliomas are the most common primary cerebral neoplasm and the major cause of morbidity and mortality in adults, with malignancy that ranges from low grade to anaplastic and glioblastoma multiforme (GBM). Histopathology is the gold standard for grading of glioma although suffers from inherent sampling error associated with stereotactic biopsy and is unable to evaluate residual tumor tissue after

cytoreductive surgery [1]. Magnetic resonance imaging (MRI) has played a significant role in noninvasive detection and classification of gliomas; however, the conventional MRI methods mostly fail to discriminate GBMs from solitary metastases [2, 3] or other glioma grades [4], and for this reason, MR measures reflecting structure and tissue function, such as in vivo MR spectroscopy (MRS), diffusion tensor imaging (DTI), and dynamic susceptibility contrast as well as dynamic contrast-enhanced (DCE) perfusion-weighted imaging (PWI) have been investigated for glioma classification [4–8].

Proton MR spectroscopy (^{1}H-MRS) enables evaluation of brain metabolites such as *N*-acetylaspartate (NAA), total choline (Cho), and total creatine (Cre). Additional signals include lactate, which becomes visible in the presence of anaerobic metabolism, and lipids, which may be observed in regions of cellular breakdown caused by necrosis. Typical characteristics of elevated Cho, decreased NAA, and the presence of lipids and lactate have been shown to be useful in tumor grading, although reports indicate a range of specificity and sensitivity levels [1, 9–11]. While many of these previous studies were performed using single-voxel spectroscopy or multi-voxel single-slice spectroscopic imaging (MRSI) with point-resolved spectroscopy (PRESS) volume selection, there are no previous reports that have used a more recently developed method of whole-brain volumetric MRSI, and there have been only a limited number of studies carried out at the increasingly available field strength of 3 T. A secondary aim of this study is to evaluate the potential advantage of obtaining metabolite maps that cover a larger volume of the cerebrum.

DTI is sensitive to the rate and direction of diffusion of water within the tissue. Studies have shown that DTI reveals larger peritumoral abnormalities in gliomas, which are not apparent on conventional MRI, and that fractional anisotropy (FA) [12–14] and apparent diffusion coefficient (ADC) have been shown to distinguish high-grade from low-grade tumors [5]. DCE-MRI measures a composite of tumor perfusion, vessel permeability, and extravascular-extracellular space volume, volume transfer coefficient (k^{trans}), rate transfer constant between the extracellular extravascular space and the plasma (k_{ep}) leakage (v_e), and plasma volume (v_p). These pharmacokinetic indices of DCE-MRI provide quantitative measurement of the integrity of the blood–brain barrier and of tissue perfusion. Several studies have shown that DCE can characterize different grades of glioma based on these hemodynamic and pharmacokinetic indices [7, 15, 16].

Information gained from these multiparametric imaging techniques is largely complementary, and combinations of these methods have been investigated for glioma classification [4, 9, 10], and their efficacy was characterized in terms of the sensitivity, specificity, positive predictive value (PPV), and negative predictive value (NPV). Studies have shown that relative cerebral blood volume (rCBV) measurements and metabolite ratios both individually and in combination can increase the sensitivity and PPV when compared with conventional MRI alone in determining glioma grade [1, 4]. In this study, our primary aims were to evaluate sensitivity, specificity, PPV, and NPV of perfusion MRI, whole-brain MRSI, and DTI for glioma grading and to determine which technique or combination of techniques is of value for classification of low- from high-grade glioma.

Materials and methods

Eighty-seven treatment-naïve patients (61 men and 26 women, aged 14–69 years) who had received a preliminary diagnosis from an experienced radiologist of intracranial space-occupying lesion on CT/MRI were included in this study. Thirteen were subsequently excluded as they were confirmed as non-gliomas on histopathology. Five studies were dropped due to motion in the data set; seven, because of low quality of spectral data in the region of the tumor; and another six were excluded due to incomplete study data where either the perfusion imaging, T2-weighted MRI, or the DTI was not available. Hence, a total of 56 patients were considered for analysis. The institutional ethics committee and the research committee approved the study protocol, and informed consent was obtained from the patients or their care providers.

MR imaging

Subjects underwent an hour-long MR protocol that included conventional MRI, whole-brain MRSI, DTI, and DCE-MRI on a 3-T Signa HDxt MRI scanner (General Electric, Milwaukee, WI) using a 12-channel head coil. Conventional imaging included T2-weighted fast spin echo (FSE) with echo time (TE)/repetition time (TR) of 101.8/3,500 ms, a signal average (NEX) of 1, field of view (FOV) of 260×260 mm^2, and 3 mm slice thickness without any interslice gap and a T1-weighted image fast spoiled gradient-recalled (FSPGR) echo with TE/TR/NEX = 3.01/8.02 ms/1, FOV of 256×256 mm^2, and 1 mm slice thickness.

MRSI data were obtained using a volumetric spin-echo MRSI sequence with echo-planar readout and TR/TE = 1,710/70 ms, FOV = 280×280×180 mm^3, 100 [read]×50 [phase]×18 [slice] spatial samples over a 135-mm slab, and acquisition time of 26 min. This included frequency-selective water suppression and inversion recovery nulling of the lipid signal with inversion time = 198 ms. This sequence included both a spin-echo excitation for the metabolite signal and a low flip-angle gradient-echo excitation for a water reference MRSI signal, which was acquired in an

interleaved fashion. The FSPGR BRAVO and MRSI acquisitions were performed at the same angulation, with the slice or slab orientations of all acquisitions parallel to the anterior commissure–posterior commissure (AC-PC) plane, or angulated at +15° from the AC-PC, which was found to facilitate improved magnetic field homogeneity over a larger volume of the cerebrum.

MRSI data were processed using the Metabolite Imaging and Data Analysis System package [17]. Metabolite image reconstruction included spatial smoothing and interpolation to 64×64×32 voxels, with a resultant voxel volume of approximately 1 mL. The automated spectral fitting of relative metabolite concentration resulted in maps for NAA, Cre, Cho, and lactate, although due to the spectral overlap with lipid signals that cannot be fully resolved by the spectral analysis procedure this, latter result is termed lactate + lipid (LL). Additional maps were obtained for the metabolite ratios and measures of spectral quality, including spectral linewidth and Cramer–Rao bounds. Individual metabolite values are reported in institutional units, and metabolite ratio values indicate the relative concentrations and not the widely reported area under the spectral peak. The processing steps included manual creation of a mask that delineated the tumor and surrounding edema; calculation of the MRSI voxel tissue content based on a four-compartment tissue segmentation of the high-resolution T1-weighted MRI into gray and white matter, cerebrospinal fluid, and an "other" tissue category; and normalization of the fitted metabolite signals to institutional units using the water reference MRSI. The signal normalization assumed a fixed water content and T1 for each tissue type to derive the 100 % water equivalent signal; however, because the water content and T1 in the tumor region is unknown, these were estimated by deriving a bias field correction map that minimized image intensity variations over the tumor region, and the resultant image used for intensity scaling was smoothed to minimize the effect of local signal variations.

DTI data were acquired using a dual spin-echo single-shot echo-planar sequence with ramp sampling, TR/TE/FOV/NEX/slice thickness/interslice gap = 10 s/100 ms/240 mm/1/3 mm/0, 46 slices, image matrix = 256×256, and diffusion-weighting b-factor of 1,000 s/mm^2 applied in 12 directions in addition to the reference measurement with b=0 s/mm^2. DTI data were processed using in-house developed software to obtain eigenvalues (λ_1, λ_2, and λ_3) and three orthonormal eigenvectors (e_1, e_2, and e_3) [18]. The tensor field data were then used to compute the DTI metrics such as ADC and FA for each voxel [18].

DCE-MRI was performed using a three-dimensional spoiled gradient-recalled (SPGR) echo sequence (TR/TE/flip angle/NEX/slice thickness/FOV/matrix size = 5.0 ms/2.1 ms/10°/0.7/6 mm/240×240 mm/128×128 mm, number of phases 32). At the start of the fourth acquisition, Gd-DTPA-BMA (OmniScan; GE Healthcare, Piscataway, NJ) was administered through a power injector (Mallinckrodt OptiStar LE) at 5 mL/s and a dose of 0.2 mmol/kg body weight, followed by a 30-mL saline flush. A series of 384 images over 32 time points for 12 slices were acquired (temporal resolution 5.65 s). Before three-dimensional SPGR, two inversion recovery FSE images (TR/TE/NEX/-slice thickness/FOV/matrix size = 940/8 ms/0.75/6 mm/240×240 mm^2/128×128 mm) with inversion times of 800 and 1,600 ms were acquired for the same slice position to quantify the voxel-wise tissue longitudinal relaxation time, T_{10}. Voxel-wise tissue longitudinal relaxation time, T_{10}, was calculated from the two inversion recovery sequences indicated above [7]. The absolute tissue T_{10} value was used to generate a concentration time curve from a signal intensity–time curve obtained from 3D FSPGR sequence using in-house developed Java-based software [7]. Quantitative analysis of the concentration–time curve was performed to calculate the CBV and a corrected CBV map generated by removing the contrast agent leakage effect due to the disrupted blood–brain barrier [18, 19]. The pharmacokinetic model was implemented for calculation of k^{trans} (in minute), k_{ep} (in minute), v_{e}, and v_{p} [7]. The relative CBV was then obtained by dividing the mean value of CBV in specified region of interest (ROI) by the value obtained from a ROI placed on the normal contralateral side of the brain.

A post-contrast T1-weighted image (FSPGR BRAVO) with TE/TR/NEX = 2.98/7.79 ms/1 was acquired with FOV of 256×256 mm^2 and 1 mm slice thickness after the acquisition of the perfusion MR imaging data. The metabolite maps, DTI metrics, and DCE-derived CBV map were co-registered. Image values were then obtained for all image types according to the following methods. For the metabolite maps, ROIs were placed within the lesion corresponding to the maximal Cho signal and minimal NAA + Cre and from contralateral normal-appearing white matter (NAWM). Mean values of NAA, Cre, Cho, and LL in the tumor and Cre and Cho in the NAWM ($\text{Cre}_{\text{Normal}}$ and $\text{Cho}_{\text{Normal}}$, respectively) were recorded from 12 interpolated voxels at each ROI, corresponding to a tissue volume of approximately 2 mL. The values of $\text{Cre}_{\text{Tumor}}/\text{Cre}_{\text{Normal}}$ and $\text{Cho}_{\text{Tumor}}/\text{Cho}_{\text{Normal}}$ ratio were then calculated for each tumor ROI. Initial evaluation indicated that all studies included voxels with zero NAA; therefore, results were not obtained for the widely reported maximum Cho/NAA ratio. If LL was present, it was confirmed that this was also present in the tumor ROIs. Values were accepted only if the fitted spectral linewidth was less than 13 Hz, and the Cramer–Rao bound for any one of NAA, Cre, and Cho was under 10 %. Since the initial analysis indicated that regions of zero metabolite signal were observed for both necrotic tissue regions and cystic tumor regions, which could be readily distinguished based on the T2 image, an additional image metric obtained

from the intensity of the T2-weighted MRI relative to the value in contralateral white matter was also included. For the DTI metrics (FA and ADC), mean values were obtained for ROIs corresponding to regions with high FA and low MD values, and for the DCE-derived rCBV, k^{trans}, k_{ep}, v_e, and v_p maps, the values were obtained for ROI corresponding to maximum corrected CBV. For each DTI-derived metrices and DCE-derived CBV maps, the values were recorded from 12 interpolated voxels at each ROI corresponding to a tissue volume of approximately 2 mL. Five ROIs were placed at five different slices of tumor, and the region showing the worst values was considered. ROIs for spectral maps were placed at different locations compared those of perfusion and diffusion maps as the region with high choline and minimal NAA + Cre did not always correspond to the region with high CBV, high FA, and low MD, and vice versa.

In addition to obtaining metabolite values normalized using tissue water, these values were also obtained using normalization with contralateral values obtained from normal-appearing white matter. Similarly, contralateral white matter CBV was obtained for determination of rCBV.

An experienced radiologist who was blinded to the MR perfusion, DTI, and MR spectroscopic results reviewed the conventional MR images and graded each tumor according to the two-tier imaging grading system: low- versus high-grade gliomas. The grading was based on the following: tissue contrast enhancement, border definition, mass effect, signal intensity heterogeneity, hemorrhage, necrosis, degree of edema, involvement of the corpus callosum, and tumor crossing the midline [1].

To evaluate the potential for whole-brain MRSI and the multiplane DCE sequence to sample lesions throughout the cerebrum, the number of studies for which the MRI-observed tumor volume was considered to be well, partially, or inadequately sampled by the MRSI or DCE study was recorded. For full sampling, this evaluation required that >75 % of the lesion volume, as indicated by the post-contrast T1- and T2-weighted images, was obtained with a sufficiently good spectral linewidth based on visual analysis.

Statistical analysis

Sample size estimation

The sensitivity and specificity of the imaging results were calculated using receiver-operating characteristic (ROC) analysis. To estimate the sample size required for this analysis, it was assumed that the area under the ROC curve under the null hypothesis will be 0.8; under the alternate hypothesis, it will be 0.99; and that the ratio between the standard deviation of responses in the positive and negative groups was 1. For 90 % power and a 0.05 level of significance, the minimum sample size required for positive and negative responses was 16 each. The data were assumed as discrete responses having binary outcome (as high or low grade).

ROC curve analyses were first used to determine the cutoff values of individual imaging metrics, with the histologically confirmed grades taken as a gold standard. Optimal threshold values were obtained by (1) minimizing the observed number of tumors misclassified (C2 error = fraction of misclassified tumors) and (2) maximizing the average of the observed sensitivity and specificity (C1 error = 1 − (sensitivity +specificity)/2). Based on these, sensitivity, specificity, PPV, and NPV were calculated for characterization of gliomas into high and low grade. To obtain the sensitivity, specificity, PPV, and NPV for combination of rCBV, metrices of diffusion tensor imaging, and spectral maps, logistic regression was performed using forward likelihood ratio method based on threshold values obtained from ROC curve analyses for each imaging measure in glioma grading.

Results

Of 56 subjects included in the study, histopathology indicated 32 with high-grade glioma (9 anaplastic astrocytoma grade III, 3 anaplastic oligoastrocytoma grade III, and 20 glioblastoma multiforme grade IV) and 24 with low-grade glioma (13 astrocytoma grade II, 7 oligodendroglioma grade II, and 4 oligoastrocytoma grade II). Contrast enhancement was seen in 35, 89, and 100 % of grades II, III, and IV tumors, respectively. In Figs.1 and 2, there are example images and spectra for a GBM where findings include the absence of NAA (Fig. 1c) over much of the T2-hyperintense region, which extends outside of the volume indicated by the T1 contrast enhancement, together with reduced Cre and strong increase of Cho. Increased LL, which was visually attributed to be primarily a representative of lactate, can be seen (Figs. 1e and 2b) within the central region. Results also show decreased FA and locally increased CBV. This result also demonstrates the ability of the whole-brain MRSI method to sample a wide volume of the brain, including the cortical surface at the position of the tumor.

MRSI results of grade II astrocytoma (Fig. 3) demonstrate an absence of NAA and reduced Cre, similar to the previous example, together with a moderate increase of Cho and a region with high lactate. The findings include increased ADC and decreased FA and CBV that are confined to the region indicated by altered T1 and T2 contrast.

Based on radiologist's reading, conventional MRI could discriminate low-grade glioma from high grade with sensitivity, specificity, PPV, and NPV as 84, 67, 77, and 76 %,

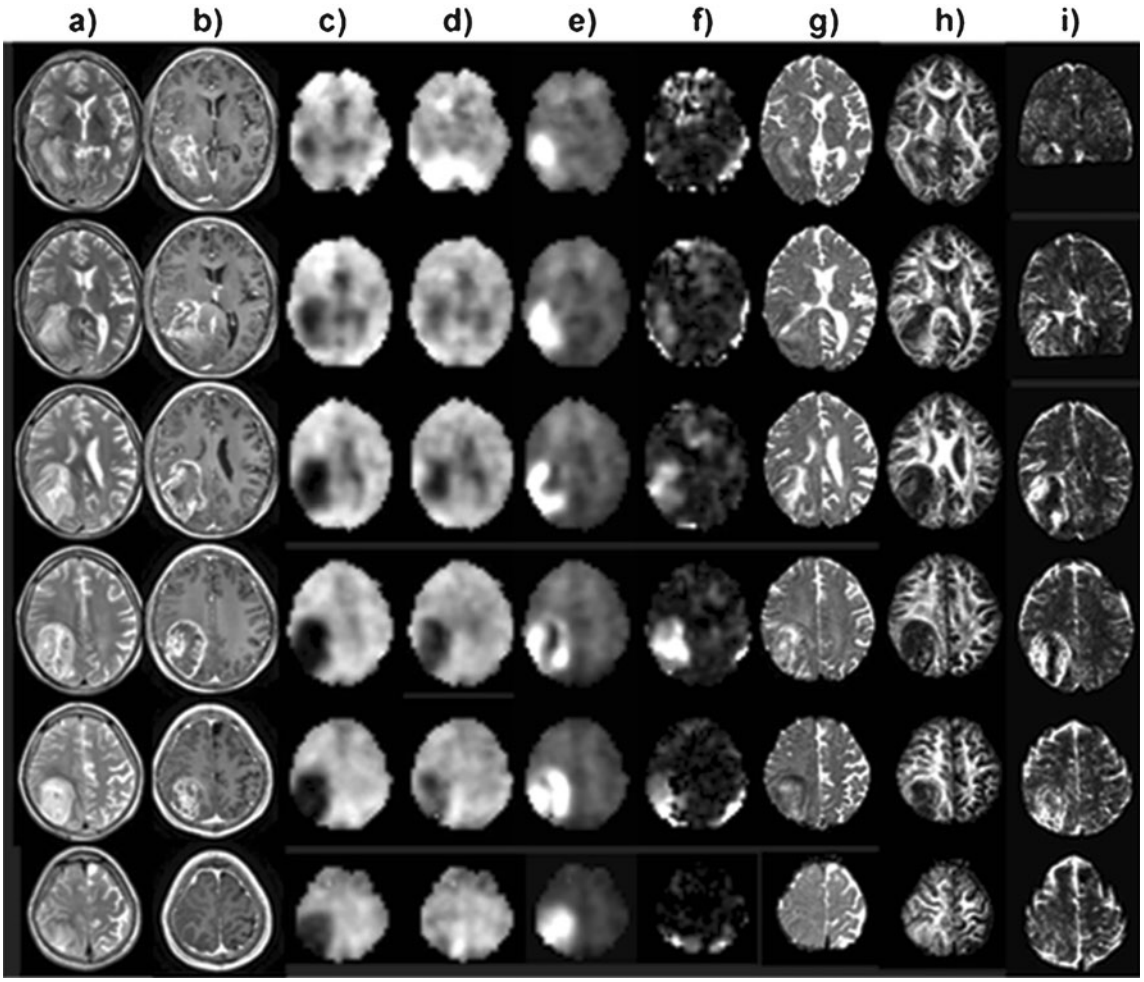

Fig. 1 Example multiparametric results for a grade IV glioblastoma multiforme in the right parietal region of a 48-year-old male subject. Multi-slice axial images are shown that correspond to every second slice of the volumetric MRSI study, at 11.2-mm spacing. *Each column* shows results for **a** T2-weighted MRI, **b** post-contrast T1-weighted MRI, **c** NAA, **d** Cre, **e** Cho, **f** LL, **g** ADC, **h** FA, and **i** CBV

respectively, with minimum C1 and C2 error as 24 and 23 %, respectively. For parameters obtained from T2-weighted FSE, DTI, DCE-MRI, and whole-brain MRSI, threshold values were obtained separately for minimum C1 and C2 error and are shown in Tables 1, 2, 3, and 4. The best performance for a single imaging measure was obtained for rCBV, for which minimum C1 and C2 error was obtained with a threshold value of 3.34 and provided sensitivity and specificity of 100 and 88 %, respectively (Table 1). Since oligodendrogliomas are known to influence the CBV values, we also analyzed the data by removing them. On removal of seven pure oligodendrogliomas from low grade and at cutoff value of 3.34 rCBV, we obtained sensitivity and specificity of 100 % each for classification of glioma grade. Oligoastrocytoma with 25 % of oligo component in our analysis was considered to be astrocytoma.

The combination of spectral parameter, rCBV, FA, ADC, and $T2_{Tumor}/T2_{Normal}$ where ROIs were placed on region with high choline resulted in sensitivity, specificity, PPV, and NPV of 100, 88, 91, and 100 %, respectively, for minimum C1 as well as C2 error. When ROIs were placed on region with minimal NAA and creatine, the combination of spectral parameter, rCBV, FA, ADC, and $T2_{Tumor}/T2_{Normal}$ provided sensitivity, specificity, PPV, and NPV of 100, 96, 97, and 100 %, respectively, for minimum C1 as well as C2 error (Table 5).

The MRSI data showed a considerable overlap of spectral characteristics across all tumor grades, with 97 % of studies having a region with no NAA signal and 68 % (58, 50, and 88 % for grades II, III, and IV, respectively), indicating the presence of lactate, as confirmed by visual identification of the lactate doublet in the spectra. Of 61 studies for which MRSI data were suitable for evaluation, the extent to which the whole-brain MRSI acquisition sampled the tumor volume with adequate quality indicated that 72 % of the studies provided >75 % coverage of the tumor and 20 % of studies sampled between 25 and 75 % of the tumor volume.

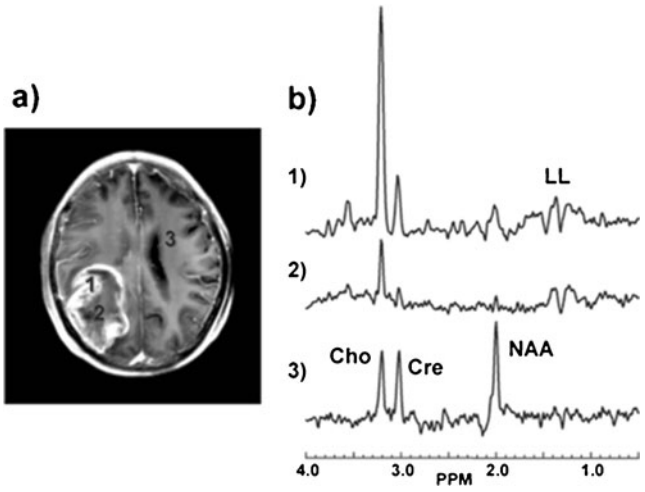

Fig. 2 Example spectra corresponding to the GBM study shown in Fig. 1. The locations of the selected spectra are indicated on the post-contrast T1 MRI (**a**) which has been integrated over ten 1-mm slices to correspond to the slice thickness of the MRSI study. The spectra (**b**) correspond to regions of *1* highest Cho, *2* smallest NAA + Cre, and *3* normal-appearing white matter

Discussion

The major finding of this study is that a combination of parameters from DCE-MRI, DTI, and whole-brain MRSI enables classification of gliomas into high and low grade with accuracy near to the classification based on histopathology. Results suggest that DCE-MRI-derived rCBV is most efficient in the classification of high-grade glioma from low grade as compared to DTI-derived metrices and spectral maps obtained from whole-brain MRSI.

Several reports have demonstrated the advantages of multiparametric MR measures for evaluation of gliomas at 1.5 and 3 T [9, 10, 14, 20]. Di Costanzo et al. [10] have shown that multiparametric MR assessment of glioma, based on ^{1}H-MRSI, PWI, and diffusion-weighted imaging, can discriminate high- from low-grade gliomas and infiltrating tumor from surrounding vasogenic edema or normal tissues. Catalaa et al. [9] evaluated perfusion, diffusion, and spectroscopy values in enhancing and non-enhancing lesions for patients with newly diagnosed gliomas of different grades to find increased cell density and increased vascularity within enhancing lesions and increased cellularity in non-enhancing region. However, these studies did not evaluate the ability to classify gliomas into low and high grade using quantitative threshold values based on ROC analysis. Analyses of single imaging measures as well as multiparametric combinations have been used for this purpose. For studies carried out at 3 T, MRS had been evaluated for grading of cerebral gliomas at different TE values [11], and ROC analysis was conducted for glioma classification using pharmacokinetic indices [16]. Combination of mean FA and maximal FA in grading of preoperative non-enhancing gliomas has been reported to discriminate low and high grade with specificity of 92.3 % and sensitivity of 86.7 % [14]. DCE-MR and spectroscopic imaging were

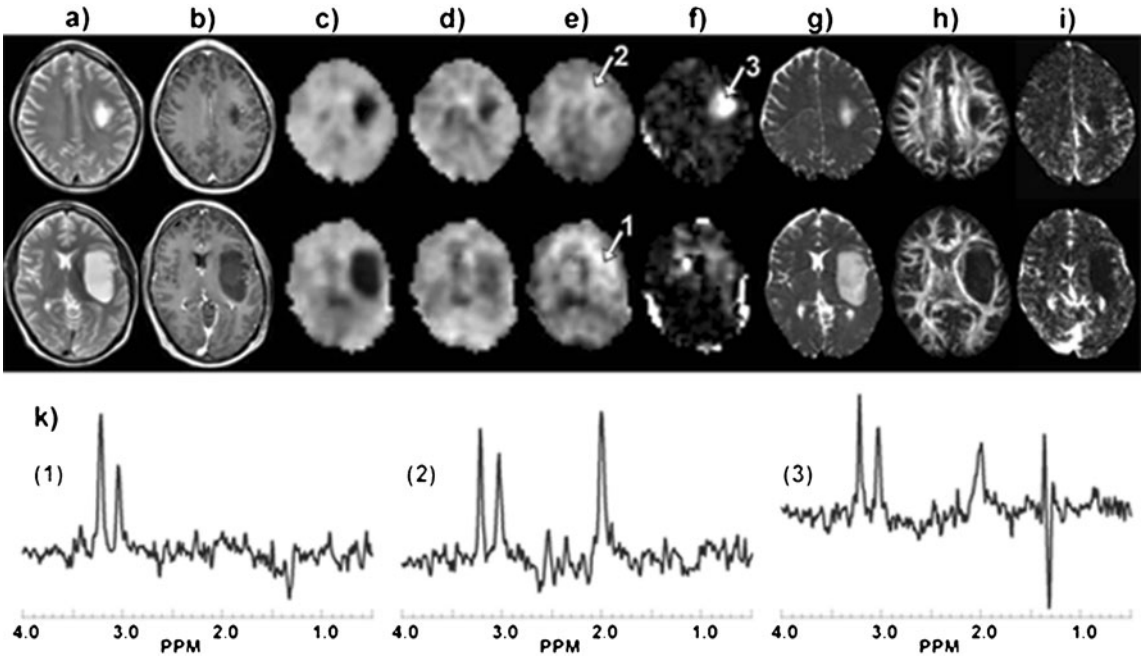

Fig. 3 Example images and spectra at two slices of 35-year-old male for a left insular grade II astrocytoma. Results are shown for **a** T2-weighted MRI, **b** post-contrast T1-weighted MRI, **c** NAA, **d** Cre, **e** Cho, **f** LL, **g** ADC, **h** FA, and **i** CBV. In **k**, sample spectra are shown, corresponding to the number regions indicated in **e** and **f**, with spectral assignments as shown in Fig. 2b

Table 1 Threshold values of DCE-derived CBV and DTI metrics for differentiating between low- and high-grade gliomas by placing ROIs on areas with maximum CBV, maximum FA, and minimum ADC

Parameters	Based on minimum C1 error					Errors		Based on minimum C2 error					Errors	
	Threshold	Sensitivity	Specificity	PPV	NPV	C1	C2	Threshold	Sensitivity	Specificity	PPV	NPV	C1	C2
rCBV	3.34	1.0	0.88	0.91	1	0.06	0.05	3.34	1.0	0.88	0.91	1	0.06	0.05
rCBV[a]	3.34	1.0	1.0	1	1	0.00	0.00	3.34	1.0	1.0	1	1	0.00	0.00
FA	0.30	0.91	0.71	0.80	0.85	0.19	0.18	0.28	0.94	0.67	0.79	0.89	0.20	0.18
ADC	0.00098	0.94	0.75	0.83	0.90	0.16	0.14	0.00098	0.94	0.75	0.83	0.90	0.16	0.14

[a] rCBV obtained after removal of seven pure oligodendrogliomas

Table 2 Threshold values of various metabolites for differentiating between low- and high-grade gliomas by placing ROIs on areas with minimum creatine and minimum NAA

	Based on minimum C1 error					Errors		Based on minimum C2 error					Errors	
	Threshold	Sensitivity	Specificity	PPV	NPV	C1	C2	Threshold	Sensitivity	Specificity	PPV	NPV	C1	C2
tCho	2,215.32	0.78	0.42	0.64	0.59	0.40	0.38	2,215.32	0.78	0.42	0.64	0.59	0.40	0.38
tCre	4,847.01	0.66	0.79	0.81	0.63	0.28	0.28	5,365.19	0.72	0.71	0.77	0.65	0.29	0.28
NAA	2,979.04	0.66	0.67	0.72	0.59	0.34	0.34	3,302.88	0.72	0.58	0.70	0.61	0.35	0.34
Cho/Cr	0.49	0.75	0.62	0.73	0.65	0.31	0.30	0.39	0.94	0.42	0.68	0.83	0.32	0.28
Lactate	3,666.28	0.78	0.58	0.71	0.67	0.32	0.30	3,666.28	0.78	0.58	0.71	0.67	0.32	0.30
CreT/CreN	0.41	0.56	0.79	0.78	0.58	0.32	0.34	0.41	0.56	0.79	0.78	0.58	0.32	0.34
ChoT/ChoN	0.57	1	0.42	0.70	1	0.29	0.25	0.57	1	0.42	0.70	1	0.29	0.25
T2T/T2N	1.73	0.94	0.62	0.77	0.88	0.22	0.20	1.73	0.94	0.62	0.77	0.88	0.22	0.20

Table 3 Threshold values of various metabolites for differentiating between low- and high-grade gliomas by placing ROIs on areas with high choline

Parameters	Based on minimum C1 error					Errors		Based on minimum C2 error					Errors	
	Threshold	Sensitivity	Specificity	PPV	NPV	C1	C2	Threshold	Sensitivity	Specificity	PPV	NPV	C1	C2
tCho	5,704.98	0.69	0.58	0.69	0.58	0.36	0.36	3,662.43	1.00	0.21	0.63	1.00	0.40	0.34
tCre	8,954.16	0.47	0.79	0.75	0.53	0.37	0.39	8,954.16	0.47	0.79	0.75	0.53	0.37	0.39
NAA	3,858.13	0.38	0.83	0.75	0.50	0.40	0.43	11,670.49	0.94	0.08	0.58	0.50	0.49	0.43
Cho/Cr	0.87	0.34	1.00	1.00	0.53	0.33	0.38	0.52	0.69	0.62	0.71	0.60	0.34	0.34
Lactate	4,580.80	0.62	0.58	0.67	0.54	0.40	0.39	2,650.64	0.88	0.29	0.62	0.64	0.42	0.38
CreT/CreN	1.26	0.31	0.96	0.91	0.51	0.36	0.41	1.14	0.34	0.92	0.85	0.51	0.37	0.41
ChoT/ChoN	2.13	0.69	0.88	0.88	0.68	0.22	0.23	1.76	0.88	0.62	0.76	0.79	0.25	0.23
T2T/T2N	1.59	0.94	0.58	0.75	0.88	0.24	0.21	1.59	0.94	0.58	0.75	0.88	0.24	0.21

Table 4 Threshold values of DCE-derived k^{trans}, k_{ep}, v_e, and v_p for differentiating between low- and high-grade gliomas by placing ROIs on areas with maximum CBV

Parameters	Based on minimum C1 error					Errors		Based on minimum C2 error					Errors	
	Threshold	Sensitivity	Specificity	PPV	NPV	C1	C2	Threshold	Sensitivity	Specificity	PPV	NPV	C1	C2
k^{trans} (min^{-1})	0.00013	0.84	0.56	0.73	0.72	0.30	0.27	0.00013	0.84	0.56	0.73	0.72	0.30	0.27
k_{ep} (min^{-1})	0.0015	0.84	0.65	0.77	0.75	0.25	0.24	0.0015	0.84	0.65	0.77	0.75	0.25	0.24
v_e	0.105	0.38	0.96	0.92	0.52	0.33	0.38	0.00035	0.56	0.74	0.75	0.55	0.35	0.36
v_p	0.017	0.59	0.96	0.95	0.63	0.22	0.25	0.0065	0.75	0.78	0.83	0.69	0.23	0.24

Table 5 tCho, tCre, NAA, Cho/Cr, lactate, CreT/CreN, ChoT/ChoN, T2T/T2N, rCBV, FA, and ADC together for differentiating between low- and high-grade gliomas

ROIs placed on region with	Threshold based on minimum C1 error				Errors		Threshold based on minimum C2 error				Errors	
	Sensitivity	Specificity	PPV	NPV	C1	C2	Sensitivity	Specificity	PPV	NPV	C1	C2
High choline	1.0	0.88	0.91	1	0.06	0.05	1.0	0.88	0.91	1	0.06	0.05
Low NAA and low creatine	1.00	0.96	0.97	1	0.02	0.02	1.00	0.96	0.97	1	0.02	0.02

combined to obtain specificity and sensitivity as 93.3 and 60.0 %, respectively, to discriminate high- and low-grade glioma [1].

Zonari et al. [4] evaluated the combined role of single-voxel MR spectroscopy, diffusion imaging, and echo-planar perfusion imaging. They concluded that combination of PWI and MRS with conventional MR imaging increases the accuracy of the attribution of malignancy to glial neoplasms. However, the current study suggests that combination of all the parameters will enhance the accuracy towards classification of glioma grade. Arvinda et al. [5] have classified gliomas using diffusion and perfusion imaging; however, they did not combine these techniques to classify high- and low-grade gliomas. Hlaihel et al. [6] studied the predictive value of multimodality MRI using conventional, perfusion, and spectroscopy MR in anaplastic transformation of low-grade oligodendrogliomas and concluded that MRS should be recommended in the follow-up of low-grade gliomas as they observed that choline/creatine ratio could predict anaplastic transformation before perfusion abnormalities, with high positive predictive value of 83 %.

In the present study, conventional MRI was able to classify gliomas into low and high grade with a sensitivity and specificity of 84 and 67 %, respectively, which is consistent with the previous studies [1, 21]. Contrast enhancement was seen in 35, 89, and 100 % of grades II, III, and IV tumors, respectively, which is consistent with earlier studies [22–24]. Among all the parameters considered, rCBV most efficiently characterized the grades with high sensitivity and specificity and minimal error, which can be due to better resolution of perfusion data as compared to spectral maps and inconsistent FA and ADC values for high- and low-grade glioma. Previous studies have indicated that functional physiological parameters like CBV and other perfusion indices have fared better than MR spectroscopy [1], which gives insight into the tissue metabolism, and indices of DTI [5], which reflect the cellular microenvironment. Several studies have reported a robust correlation between microvascular density and tumor grade [25], which supports the association of rCBV with tumor grade. Additional considerations of choice of imaging method include the lack of standardization of MRS acquisition and quantification methods, and variability of the measurements, leading to decreased sensitivity and specificity relative to MR perfusion.

In this study, rCBV cutoff value of 3.34 resulted in a sensitivity and specificity of 100.0 and 88.0 %, respectively, was observed, which is consistent with previous reports [5, 26]. However, Law et al. [1] reported a threshold value of 1.75, for a sensitivity, specificity, PPV, and NPV of 95.0, 57.5, 87.0, and 79.3 %, respectively. This difference in the threshold value may be due to the larger variation in the rCBV values for high-grade glioma and the technique used for quantification of rCBV in the study of Law et al., which resulted in the lower specificity as compared to the present study. The separate analysis of the data after removal of seven oligodendrogliomas improved the sensitivity and specificity to 100 %, indicating that the presence of oligodendrogliomas does influence the glioma grading. This is probably due to the difference in the vascular profile of these two different types of tumors and their inherent dense network of branching capillaries which resembles to "chicken wire" pattern [14, 27].

Earlier study showed that k_{ep} and v_e, together with rCBV, classified 100 % of low-grade tumors and 89.1 % of high-grade tumors correctly [7]. The k^{trans} and v_e are shown to discriminate high from low grade with good sensitivity and specificity [16] similar to our results. However, the current study suggests that the pharmacokinetic indices k^{trans}, k_{ep}, v_e, and v_p are not as sensitive and specific in the classification of glioma as rCBV since it provides with higher sensitivity and specificity.

For regions with minimal NAA + Cre, the ratio of T2 signal intensity to that of normal contralateral white matter and creatine was also relatively effective for classification of glioma, as compared to the other metabolite maps obtained. ROIs placed on regions with maximal Cho gave the ratio of the T2 MRI signal intensity in the tumor to normal contralateral white matter and Cho_{Tumor}/Cho_{Normal} as the most effective classifier. The combination of rCBV, FA, ADC, and spectroscopic parameters was able to discriminate high and low grade with only 6 and 5 % of C1 and C2 error, respectively, when ROIs were placed in region with

maximum rCBV, FA, ADC, and choline. Combinations of the same parameters obtained from ROIs placed in regions with maximum rCBV, FA, ADC and minimal NAA + Cre were able to discriminate high and low grade with 2 % of C1 and C2 error and sensitivity and specificity as 100 and 96 %, respectively. This considerable improvement in discrimination between grades is due to the complementary information provided from perfusion-weighted, diffusion-weighted, and spectroscopic parameters, and this adds value to clinical diagnosis for differentiating primary glioma.

This is the first study evaluating the whole-brain MRSI method for tumor characterization. The availability of the volumetric MRSI measurement with relatively good spatial resolution provided sufficient coverage of the brain with 92 % of the studies analyzed considered to have sampled a portion of the tumor volume considered sufficient to make a ROI-based measurement. A potential benefit of the improved spatial sampling and relatively good resolution over conventional PRESS volume-selected MRSI methods is improved accuracy for ROI selection. Nevertheless, the diagnostic performance of the MRSI method used in this study remains comparable to previous reports carried out at 1.5 T using two-dimensional PRESS volume-selected MRSI [1] and reporting metabolite ratios. In comparison to the study of Law et al. [1] for Cho/Cre, this study shows comparable sensitivity and a small improvement in specificity. An additional observation is that the use of signal-normalized individual metabolite values resulted in a diagnostic performance similar to that obtained from the Cho/Cre or using normalization by the values in contralateral while matter.

A new finding of this study is the potential of Cre as a diagnostic marker. Although widely used as a concentration standard, there is regional and individual variability in concentration [28], and it has been shown to be decreased in tumors [29]; however, higher Cre values relative to NAWM values were associated with shorter survival [30]. The results of this study indicate that when ROIs were selected based on minimum creatine and NAA, the classifications based on either the signal-normalized Cre or that normalized to the value in NAWM achieved the highest specificity of the MRS measures.

This study addresses the known limitation of taking metabolite ratios to Cre, and a remaining limitation is that the signal normalization did not included measured water density and T1 values, for which alterations from normal values could affect measurements both within the tumor or NAWM. It is, however, notable that performance for Cho alone was poorer than that of Cho/Cre and ChoT/ChoN. Noncorrelation of the imaging values with image-guided histology of the tumor sample may be considered as another limitation of this study.

Conclusion

The results of this study demonstrate that the application of a comprehensive multiparametric MR protocol enables grading of gliomas with almost 100 % accuracy. This is likely to be due to complementary information provided from perfusion- and diffusion-weighted imaging and spectroscopic parameters. Individually, rCBV measurements provide the utmost diagnostic performance for predicting glioma grade. This multiparametric MR approach will provide physicians treating patients with primary glioma with additional diagnostic information.

Acknowledgments This work was supported in part by Indo-US Science and Technology Forum award no. 20-2009. BR received financial assistance from the University Grant Commission, New Delhi, India. RA received financial assistance from the Indian Council of Medical Research, New Delhi, India. Sequence and software development was carried out under NIH grant R01EB000822.

Conflict of interest We declare that we have no conflict of interest.

References

1. Law M, Yang S, Wang H et al (2003) Glioma grading: sensitivity, specificity, and predictive values of perfusion MR imaging and proton MR spectroscopic imaging compared with conventional MR imaging. AJNR Am J Neuroradiol 24:1989–1998
2. Chiang IC, Kuo YT, Lu CY et al (2004) Distinction between high-grade gliomas and solitary metastases using peritumoral 3-T magnetic resonance spectroscopy, diffusion, and perfusion imagings. Neuroradiology 46:619–627
3. Server A, Orheim TE, Graff BA et al (2011) Diagnostic examination performance by using microvascular leakage, cerebral blood volume, and blood flow derived from 3-T dynamic susceptibility-weighted contrast-enhanced perfusion MR imaging in the differentiation of glioblastoma multiforme and brain metastasis. Neuroradiology 53:319–330
4. Zonari P, Baraldi P, Crisi G (2007) Multimodal MRI in the characterization of glial neoplasms: the combined role of single-voxel MR spectroscopy, diffusion imaging and echo-planar perfusion imaging. Neuroradiology 49:795–803
5. Arvinda HR, Kesavadas C, Sarma PS et al (2009) Glioma grading: sensitivity, specificity, positive and negative predictive values of diffusion and perfusion imaging. J Neurooncol 94:87–96
6. Hlaihel C, Guilloton L, Guyotat J et al (2010) Predictive value of multimodality MRI using conventional, perfusion, and spectroscopy MR in anaplastic transformation of low-grade oligodendrogliomas. J Neurooncol 97:73–80
7. Awasthi R, Rathore RKS, Soni P et al (2012) Discriminant analysis to classify glioma grading using dynamic contrast-enhanced MRI and immunohistochemical markers. Neuroradiology 54:205–213
8. Moon WJ, Choi JW, Roh HG et al (2012) Imaging parameters of high grade gliomas in relation to the MGMT promoter methylation status: the CT, diffusion tensor imaging, and perfusion MR imaging. Neuroradiology 54:555–563
9. Catalaa I, Henry R, Dillon WP et al (2006) Perfusion, diffusion and spectroscopy values in newly diagnosed cerebral gliomas. NMR Biomed 19:463–475

10. Di Costanzo A, Scarabino T, Trojsi F et al (2006) Multiparametric 3T MR approach to the assessment of cerebral gliomas: tumor extent and malignancy. Neuroradiology 48:622–631
11. Kim JH, Chang KH, Na DG et al (2006) 3T ^{1}H-MR spectroscopy in grading of cerebral gliomas: comparison of short and intermediate echo time sequences. AJNR Am J Neuroradiol 27:1412–1418
12. Jolapara M, Patro SN, Kesavadas C et al (2011) Can diffusion tensor metrics help in preoperative grading of diffusely infiltrating astrocytomas? A retrospective study of 36 cases. Neuroradiology 53:63–68
13. Jakab A, Molnár P, Emri M et al (2011) Glioma grade assessment by using histogram analysis of diffusion tensor imaging-derived maps. Neuroradiology 53:483–491
14. Liu X, Tian W, Kolar B et al (2011) MR diffusion tensor and perfusion-weighted imaging in preoperative grading of supratentorial nonenhancing gliomas. Neuro Oncol 13:447–455
15. Law M, Yang S, Babb JS et al (2004) Comparison of cerebral blood volume and vascular permeability from dynamic susceptibility contrast-enhanced perfusion MR imaging with glioma grade. AJNR Am J Neuroradiol 25:746–755
16. Jia Z, Geng D, Xie T et al (2012) Quantitative analysis of neovascular permeability in glioma by dynamic contrast-enhanced MR imaging. J Clin Neurosci 19:820–823
17. Maudsley AA, Darkazanli A, Alger JR et al (2006) Comprehensive processing, display and analysis for in vivo MR spectroscopic imaging. NMR Biomed 19:492–503
18. Awasthi R, Verma SK, Haris M et al (2010) Comparative evaluation of dynamic contrast-enhanced perfusion with diffusion tensor imaging metrics in assessment of corticospinal tract infiltration in malignant glioma. J Comput Assist Tomogr 34:82–88
19. Singh A, Haris M, Rathore D et al (2007) Quantification of physiological and hemodynamic indices using T1 dynamic contrast-enhanced MRI in intracranial mass lesions. J Magn Reson Imaging 26:871–880
20. Server A, Graff BA, Orheim TE et al (2011) Measurements of diagnostic examination performance and correlation analysis using microvascular leakage, cerebral blood volume, and blood flow derived from 3T dynamic susceptibility-weighted contrast-enhanced perfusion MR imaging in glial tumor grading. Neuroradiology 53:435–447
21. Haegler K, Wiesmann M, Böhm C et al (2012) New similarity search based glioma grading. Neuroradiology 54:829–837
22. Pope WB, Sayre J, Perlina A et al (2005) MR imaging correlates of survival in patients with high-grade gliomas. AJNR Am J Neuroradiol 26:2466–2474
23. Chaichana KL, McGirt MJ, Niranjan A et al (2009) Prognostic significance of contrast-enhancing low-grade gliomas in adults and a review of the literature. Neurol Res 31:931–939
24. Lote K, Egeland T, Hager B et al (1998) Prognostic significance of CT contrast enhancement within histological subgroups of intracranial glioma. J Neurooncol 40:161–170
25. Tynninen O, Aronen HJ, Ruhala M et al (1999) MRI enhancement and microvascular density in gliomas. Correlation with tumor cell proliferation. Invest Radiol 34:427–434
26. Shin JH, Lee HK, Kwun BD et al (2002) Using relative cerebral blood flow and volume to evaluate the histopathologic grade of cerebral gliomas: preliminary results. AJR Am J Roentgenol 179:783–789
27. Narang J, Jain R, Scarpace L et al (2011) Tumor vascular leakiness and blood volume estimates in oligodendrogliomas using perfusion CT: an analysis of perfusion parameters helping further characterize genetic subtypes as well as differentiate from astroglial tumors. J Neurooncol 102:287–293
28. Maudsley AA, Domenig C, Govind V et al (2009) Mapping of brain metabolite distributions by volumetric proton MR spectroscopic imaging (MRSI). Magn Reson Med 61:548–559
29. McLean MA, Sun A, Bradstreet TE et al (2012) Repeatability of edited lactate and other metabolites in astrocytoma at 3T. J Magn Reson Imaging 36:468–475
30. Hattingen E, Delic O, Franz K et al (2010) (1)H MRSI and progression-free survival in patients with WHO grades II and III gliomas. Neurol Res 32:593–602